CROSS-LINKED NANOTUBE MATERIALS WITH VARIABLE STIFFNESS TETHERS

S. J. V. Frankland[1], G. M. Odegard[1], M. N. Herzog[2], T.S. Gates[3], C.C. Fay[4]

NASA Langley Research Center, Hampton, VA

Abstract

ASC/ASTM-D30 Joint
19th Annual Technical Conference

Atlanta, GA, October 17-20, 2004

ABSTRACT

The constitutive properties of a cross-linked single-walled carbon nanotube material are predicted with a multi-scale model. The material is modeled as a transversely isotropic solid using concepts from equivalent-continuum modeling. The elastic constants are determined using molecular dynamics simulation. Some parameters of the molecular force field are determined specifically for the cross-linker from *ab initio* calculations. A demonstration of how the cross-linked nanotubes may affect the properties of a nanotube/polyimide composite is included using a micromechanical analysis.

INTRODUCTION

Carbon nanotube composites have the potential to become light-weight, high-strength alternatives to conventional composites for aerospace applications. To

[1] Staff Scientist, National Institute of Aerospace.
[2] NRC Research Associate.
[3] Senior Materials Research Engineer, Mechanics and Durability Branch.
[4] Senior Polymer Scientist, Advanced Materials and Processing Branch.

facilitate the development of these materials, validated multi-scale models are essential to identifying the relationships between the molecular structure and the mechanical behavior of the material [1,2]. At NASA Langley Research Center, a class of cross-linked nanotube materials is being developed through a collaboration of synthesis, modeling, and characterization capabilities.

Cross-linking between nanotubes has the potential for increasing the mechanical performance of the material in nanotube based composites. Cross-linking may affect load transfer between nanotubes and dispersion of the nanotubes. To date, work has focused on the development of a short, rigid linker, and constitutive behavior of the material has been derived with a multi-scale model [3,4]. With this type of linker, some separation of the nanotubes, as well as some improvement in the transverse shear modulus over that of the non-cross-linked nanotube bundle was observed.

The objective of the present work is to use multi-scale modeling to extend previous work to investigate the effect of a more complex nanotube cross-linker on the overall constitutive properties of a nanotube/polymer composite. The modeling procedure begins with the molecular modeling of the cross-linked nanotubes using *ab initio* calculations and molecular dynamics (MD) simulations. The elastic constants of the cross-linked nanotube material are subsequently determined using an equivalent-continuum modeling technique. The elastic constants are then used in micromechanics to show the performance of a crosslinked nanotube/polyimide composite material for a range volume fractions.

MATERIAL SYSTEM

A model is developed for a cross-linked single-walled carbon nanotube material. The cross-linking material is a symmetrical di-linker which connects two nanotubes (Figure 1). It contains two stiff (chemically rigid) segments near the nanotubes and a flexible set of ether linkages in the middle segment. The atomistic structure of the cross-linking connections to the nanotubes is shown in Figure 2(a), and the molecular structure of the thermally-equilibrated system is shown in Figure 2(b). The nanotubes

are (10,10) single-walled achiral nanotubes with a radius of 6.78 Å. The atomistic structure includes 9 nanotubes which are 54 Å long.

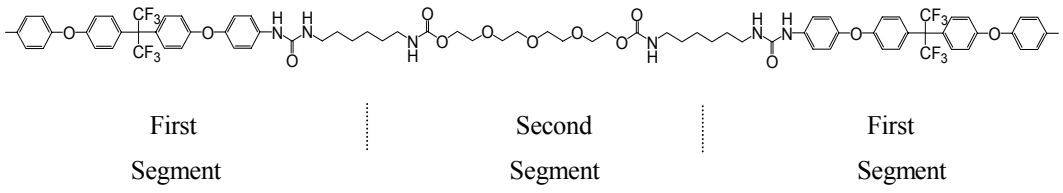

Figure 1. Variable stiffness cross-linker.

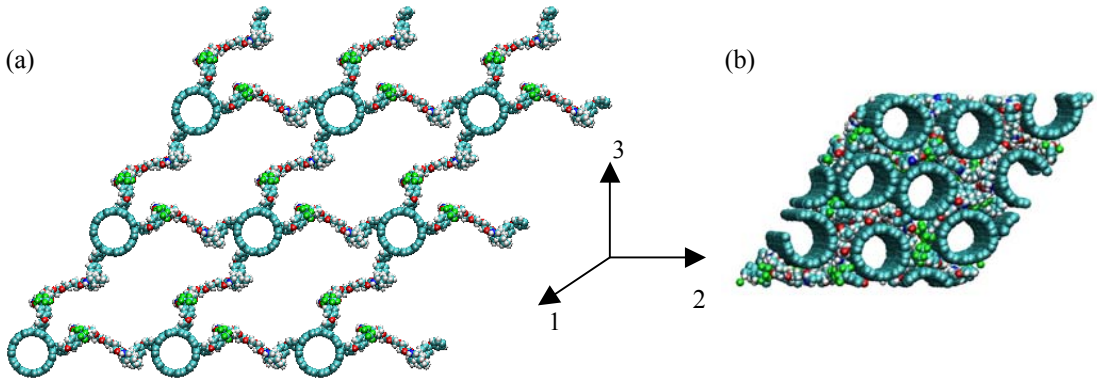

Figure 2: Molecular structure of cross-linked nanotube material and principal directions. (a) Initial structure and (b) Equilibrated structure

MULTISCALE METHOD

To predict the overall mechanical properties of a cross-linked nanotube/polymer composite material, a hierarchical multi-scale modeling procedure has been employed. First, the details of the molecular structure of the cross-linking agent are analyzed with *ab initio* calculations. This step is important because it provides the basis for an appropriate chemical structure. It generates two pieces of information: the molecular geometry of the cross-linker, and an approximation to its electronic structure. The

molecular geometry includes chemical bond lengths and angles between atoms. The electronic structure is approximated as a set of partial point charges located at the atomic position. These electronic charges also contribute directly into the strain energies used in higher levels of the model. For the cross-linking agent used in this work, the inclusion of electronic charge is especially necessary because electronegative atoms, such as nitrogen, oxygen, and fluorine, are present in the chemical structure (Figure 1).

The second step of the modeling is to derive a force field to be used in classical simulations. This step moves beyond the molecular structure to consider which molecular forces will describe the molecular interactions, and ultimately what molecular attributes will, therefore, contribute to the strain energy. The force field includes analytical functional forms for the potential energy and forces which determine how the bonds stretch, the angles bend, and what torsional motion occurs within the molecule. It also includes terms which describe the non-chemically bonded molecular interactions such as approximations to the van der Waals forces and the electronic forces. The van der Waals interactions are approximated by a Lennard-Jones potential function. The electronic charges interact via Coulomb's law.

Third, molecular dynamics simulations utilize the force field to determine the overall equilibrium molecular structure and the strain energy for the equivalent-continuum modeling. The atomistic description is necessary to determine the effects of the molecular structure, and especially, the effects of the chemical cross-linking on the strain energies. With no chemical linkers between nanotubes, the system is a nanotube bundle with van der Waals forces between the nanotubes. The strain energies are determined from the application of a displacement field to the molecular system. When a displacement field is applied to the molecular structure of the cross-linked nanotubes, there is a change in the potential energy of the molecular system which is equal to the strain energy in the equivalent continuum. For the cross-linked nanotubes, the equivalent continuum has the properties of a transversely isotropic solid. The source of the contributions to the strain energies can be broken down into the molecular interactions in the molecular dynamics simulations. Every term in the force field contributes to the potential energy, and when the system is under strain, the potential energy changes accordingly.

Fourth, the constitutive properties of an equivalent continuum are determined from strain energies computed by the molecular dynamics simulations. It is assumed that the material is transversely isotropic with its overall mechanical behavior represented with five independent elastic constants. Finally, and by way of application to composites, the constitutive properties are used to predict the mechanical properties of a polymer/nanotube composite using micromechanics to estimate the effect of embedding the cross-linked nanotubes as an effective fiber in the polymer matrix.

Quantum Chemistry

The cross-linker can be thought of as a symmetric molecule composed of two segments as shown in Figure 1. To reduce the size of the quantum *ab initio* calculations, charges were fit for each of the two segments separately, assuming hydrogen termination. The molecular geometry of each segment was optimized using a HF/STO-3G calculation [5]. This calculation minimizes the energy of the molecule in the Hartree-Fock (HF) approximation to the Schroedinger equation. The Hartree-Fock approximation does not include electron correlation terms, and it assumes only some instantaneous electron correlation. The STO-3G refers to the basis set which is the selection of atomic orbitals and their analytic form. It includes the s- and p-orbitals of the first row atoms of the periodic table and hydrogen. To fit the charges at this geometry, a larger basis set, the 6-31 G*, was used. This basis set is extended to include some d-type polarization functions for non-hydrogen atoms [5]. The charges were fit using the ESP method [5].

Having obtained charges for each atom, some modifications were made to combine the two segments to form the cross-linker. First, the charge on C-atom on the cross-linker attached to the nanotube was neutralized. This change was to avoid an unnecessarily polar bond (large charge separation) as the attached hydrogen was replaced by a nanotube atom which was assigned to be neutral. Second, at the end of the propyl groups, it was observed that the aliphatic carbon furthest away from the C=O bond had a large negative charge on it of -0.4 e. To form the hexyl group, this carbon, the adjacent one, and their associated hydrogens were neutralized. Minor

adjustments were made in the rest of the linker to accommodate these changes. All the *ab initio* calculations were performed with NWChem [6].

Force Field

The nanotube force field is based on the AMBER force field [7]. It includes energy contributions from the bond stretches, angle bends, torsions, non-bonded interactions between the 1-4 torsional interactions and non-bonded interactions with all other atoms in the system. The bonds are represented by harmonic stretches by

$$U = \tfrac{1}{2} k_b (r - r_0)^2 \tag{1}$$

where U is the potential energy, k_b is the force constant for the bond stretch, and r_0 is the bond length. These values are k_b=3924 kJ/mol [7] and r_0=1.42 Å. Similarly, the angle bends are represented by harmonic valence angle potentials of the form

$$U = \tfrac{1}{2} k_a (\theta - \theta_0)^2 \tag{2}$$

where k_a is the force constant for the angle bend and θ_0 is the equilibrium angle, parameterized as k_a=570 kJ/mol and θ_0=120° [7]. The torsions are represented as

$$U = A[1 + \cos(n\psi - d)] \tag{3}$$

where the torsional constant A=15.2 kJ/mol, the phase shift d=180°, the integer n=2 and the torsional angle is ψ [7]. Non-bonded interactions between nanotubes are represented with the Lennard-Jones potential. The parameters for this potential are given in Table I. Non-bonded interactions between 1-4 torsional partners are also included, but are scaled by 50%.

Similarly, the cross-linker and its chemical bonds to the nanotube are also represented with the AMBER force field [7]. Most of the parameters are taken directly from Ref. 7. In addition to the potential forms used for the nanotube, this

force field also includes improper torsions with the phenyl rings of the cross-linker. These interactions are represented with Eq. (3), and the parameters from Ref. 7. The cross-linker to nanotube bond was represented as by an aromatic to aliphatic C-C bond with r_0=1.53 Å. Some modifications to the force field parameterization were made. First, the Lennard-Jones interactions were simplified to include the list in Table I. This change was for convenience in setting up the force field manually in DL-POLY. Second, the partial point charges, derived for specifically for the cross-linker, from the *ab initio* calculations (described above) were used a classical approximation to the distribution of electronic charge within the molecule. While it is typical for AMBER-type force fields such as the one in Ref. 7 to include partial point charges at each atom as a classical approximation to the electronic structure of the molecule, charges are usually specific to the local chemical arrangement of molecule, and are, therefore, best derived for the particular molecular structure of interest. The charges contribute to the system potential energy, and therefore, the strain energy, via Coulomb's law. Third, the bond lengths r_0 and angles θ_0 for the cross-linker where chosen from the optimized geometry obtained from the *ab initio* calculations used in the charge-fitting procedure.

TABLE I. Lennard-Jones Parameters

Atom Type	Lennard-Jones ε_{LJ} (kJ/mol)	Lennard-Jones σ_{LJ} (Å)
C	0.3598	3.40
H	0.0628	2.60
H (from N-H)	0.0657	1.07
O	0.7950	2.98
N	0.7113	3.25
F	0.2552	3.12

Molecular Dynamics Simulations

The molecular dynamics simulations used to apply the displacement fields are started with an equilibrated structure like that in Figure 2(b). In these simulations, Newton's equations of motion are integrated to move atoms according to the intermolecular forces. The molecular structures evolve in increments of time steps

(0.5 fs). A strain level of 0.25 % is applied incrementally every 10,000 (5 ps) steps of the simulation (0.5 fs per time step). The strain is applied in the form of displacement to all the vectors describing the box shape, as well as to all the atomic coordinate vectors. The molecular structure was strained in both positive and negative directions making a total of 10 simulations to obtain five independent elastic constants. Each constant was then calculated by a parabolic fit to average potential energy over the last 3,000 steps per strain level versus strain.

To obtain the structure of Figure 2(b), molecular dynamics simulations were started with the initial structure in Figure 2(a). After a few steps to begin the equilibration process, the size of the molecular structure was gradually reduced in the transverse directions (*2* and *3* in Figure 2). This compression was done by applying strain at a rate of 0.25% per 250 steps. These simulations were performed at a constant temperature of 300 K in the microcanonical ensemble (constant NVE), only deviating to apply the displacement field which forces a change in the system volume. A second simulation was used to refine the structure before applying the displacement fields. In this simulation, the structure was further equilibrated in an isobaric-isothermal (NPT) ensemble, where all three dimensions were adjustable. The simulations were carried out with DL-POLY [8], using periodic boundary conditions. An Ewald summation was used to remove the effects of the long-range forces on the periodicity of the structure, which result from the partial charges at each atom. This step doubled the computational time.

Elastic Constants

The material system is modeled as a transversely isotropic solid. The constitutive relation is

$$
\begin{aligned}
\sigma_{11} &= C_{11}\varepsilon_{11} + C_{12}\varepsilon_{22} + C_{12}\varepsilon_{33} \\
\sigma_{22} &= C_{12}\varepsilon_{11} + C_{22}\varepsilon_{22} + C_{23}\varepsilon_{33} \\
\sigma_{33} &= C_{12}\varepsilon_{11} + C_{23}\varepsilon_{22} + C_{22}\varepsilon_{33} \\
\sigma_{23} &= G_{23}\gamma_{23} \\
\sigma_{12} &= G_{12}\gamma_{12} \\
\sigma_{13} &= G_{12}\gamma_{13}
\end{aligned}
\tag{4}
$$

where $\sigma_{ij,}$ $C_{ij,}$ and ε_{ij} are components of the stress, stiffness, and strain tensors respectively, γ_{ij} the shear strain, and i,j=1-3 [9]. The G_{12} and G_{23} are the longitudinal and transverse shear moduli, respectively. Isotropy exists in the *2-3* plane, therefore,

$$
\begin{aligned}
K_{12} &= \tfrac{1}{4}(C_{11} + 2C_{12} + C_{22}) \\
K_{23} &= \tfrac{1}{2}(C_{22} + C_{23}) \\
G_{23} &= \tfrac{1}{2}(C_{22} - C_{23})
\end{aligned}
\qquad . \tag{5}
$$

where K_{12} is the longitudinal plane strain bulk modulus and K_{23} is the transverse plane strain bulk modulus. The five independent constants $C_{11,}$ $K_{12,}$ $K_{23,}$ $G_{12,}$ and G_{23} are computed by employing displacement fields in molecular dynamics simulation. These displacement fields *u(x)* are summarized in Table II, along with the respective strain energy Λ over the system volume V. Unless the amounts of strain ε and shear strain γ are specified, the strains are zero. From the five independent constants, $C_{11,}$ $C_{12,}$ $C_{22,}$ $C_{23,}$ $G_{23,}$ and G_{13} of Eq. (4) can be determined.

TABLE II. STRAIN ENERGY AND DISPLACEMENT FIELDS

Elastic Constant	Strain Energy Equivalent	Strain	Displacement Fields
C_{11}	$\Lambda = \frac{1}{2} V C_{11} \varepsilon^2$	$\varepsilon_{11}=\varepsilon$	$u(x_1)=\varepsilon x_1$ $u(x_2)=0$ $u(x_3)=0$
K_{12}	$\Lambda = 2 V K_{12} \varepsilon^2$	$\varepsilon_{11}=\varepsilon_{22}=\varepsilon$	$u(x_1)=\varepsilon x_1$ $u(x_2)=\varepsilon x_2$ $u(x_3)=0$
K_{23}	$\Lambda = 2 V K_{23} \varepsilon^2$	$\varepsilon_{22}=\varepsilon_{33}=\varepsilon$	$u(x_1)=0$ $u(x_2)=\varepsilon x_2$ $u(x_3)=\varepsilon x_3$
G_{12}	$\Lambda = \frac{1}{2} V G_{12} \gamma^2$	$\gamma_{12}=\gamma$	$u(x_1)=\gamma x_2$ $u(x_2)=\gamma x_1$ $u(x_3)=0$
G_{23}	$\Lambda = \frac{1}{2} V G_{23} \gamma^2$	$\gamma_{23}=\gamma$	$u(x_1)=0$ $u(x_2)=\gamma x_3$ $u(x_3)=\gamma x_2$

Micromechanics

The constitutive behavior was predicted with a micromechanical analysis method. The composite material was assumed to consist of a cross-linked nanotube in a polyimide matrix. It was assumed in the micromechanical analysis that perfect bonding exists between the nanotube/polymer effective fibers and the surrounding polyimide matrix.

The micromechanics-based Mori-Tanaka method [10,11] was used to predict the elastic mechanical properties of the composite material. For this method, the overall elastic-stiffness tensor of the composite containing transverse-isotropic effective fibers embedded in an isotropic matrix material is

$$\mathbf{C} = \left(c_m \mathbf{C}^m + c_f \left\langle \mathbf{C}^f \mathbf{T}^f \right\rangle \right) \left(c_m \mathbf{I} + c_f \left\langle \mathbf{T}^f \right\rangle \right)^{-1} \tag{6}$$

where c_f and c_m are the effective fiber and matrix volume fractions, respectively, $\mathbf{C}^f$ and $\mathbf{C}^m$ are the stiffness tensors of the effective fiber and matrix, respectively, $\mathbf{I}$ is the identity tensor, the angle-brackets indicate an effective-fiber orientation average, and $\mathbf{T}^f$ is the dilute strain-concentration tensor of the effective fibers, and is given by

$$\mathbf{T}^f = \left[\mathbf{I} + \mathbf{S}^f \left(\mathbf{C}^m\right)^{-1} \left(\mathbf{C}^f - \mathbf{C}^m\right)\right]^{-1} \tag{7}$$

where $\mathbf{S}^f$ is the Eshelby tensor [12]. For three-dimensional randomly oriented effective fibers, the orientation average of a tensor, $\mathbf{A}$, is

$$\left\langle \mathbf{A} \right\rangle = \left\langle A_{ijmn} \right\rangle = \left(\kappa - \frac{2}{3}\mu\right)\left(\delta_{ij}\delta_{mn}\right) + \mu\left(\delta_{im}\delta_{jn} + \delta_{in}\delta_{jm}\right) \tag{8}$$

where $i,j,m,n = 1,2,3$; the indicial summation convention is used; δ_{ij} is the Kronecker delta; and

$$\begin{aligned} \kappa &= \frac{1}{9} A_{iijj} \\ \mu &= \frac{1}{10}\left(A_{ijij} - \frac{1}{3} A_{iijj}\right) \end{aligned} \tag{9}$$

Therefore, from Eqs. (8) and (9), $\left\langle \mathbf{A} \right\rangle$ is isotropic.

For the cross-linked, nanotube fiber/polyimide composite considered in the present study, the elastic stiffness components, volume fraction, length, and orientation of the effective fiber were used for the inclusion properties in Eq. (6). The effective fibers were assumed to have a spheroidal geometry for the Eshelby tensor. While the nanotube and effective-fiber lengths are equivalent, the nanotube volume fraction was determined to be 62.5% of the effective-fiber volume fraction. This value was calculated by assuming the nanotube volume is defined as the total space occupied by the nanotube, including half of the van der Waals separation between the

nanotube and polymer. It was assumed that the polyimide matrix was isotropic with properties equal to those of LaRC-SI [13], with a Young's modulus and Poisson's ratio of 3.8 GPa and 0.4, respectively. The overall composite stiffness was calculated for randomly-oriented effective-fibers with aspect ratios (length/diameter) of 1000 and volume fractions up to 40%.

RESULTS AND DISCUSSION

The elastic constants for the cross-linked nanotubes are included in Table 1. The lowest values, K_{23}, G_{12}, and G_{23} have the highest degree of uncertainty. The reason for the uncertainty is that these values are the most affected by the thermal noise in the simulation that arises when the potential energy change resulting from the displacement field is small compared to the potential energy change resulting from the thermal fluctuations. The uncertainty in the simulation results for C_{11} and K_{12} is much smaller, and can be estimated from standard error of the fit. For K_{12}, a standard deviation of +/- 6 GPa is estimated from the variation in the parabolic fit of strain energy versus strain. With this degree of uncertainty in mind, it is assumed that the five independently determined constants in Table III do not give a positive definite matrix (C_{12}=-16 GPa). To within 95 % confidence, K_{12} is within a range of 68-92 GPa. An arbitrary choice of K_{12}=88.6 GPa is chosen to obtain a positive definite matrix. This value is reasonable within the simulation uncertainty. With this value, the six constants in Eq. (1) become C_{11} = 350 GPa, C_{22} =3.5 GPa, C_{12} = 1.1 GPa, C_{23} = 1.9 GPa, G_{12} = 3.7 GPa, and G_{23} = 0.8 GPa.

For comparison, the elastic constants of a pure nanotube bundle (without cross-linker) with the same nanotube force field [3] are examined. The current C_{11} value is 61 % of the C_{11} value of the nanotube bundle which is close to the proportionality expected from the reduction in nanotube volume fraction (62.5% in the cross-linked nanotube fiber). The value of G_{23} also compares favorably. The current value of G_{12} is an order of magnitude lower, possibly because the flexible cross-linker is able to absorb some strain energy. The current value of K_{23} is also an order of magnitude lower, most likely because of the reduction in van der Waals attractions from the

nanotube separation in the cross-linked material. This effect was observed with a shorter cross-linker [3]. The most unusual difference is in the K_{12} value. This increase may simply be the result of packing a large amount of cross-linker between the nanotubes, therefore, contributing additional resistance to deformation in both directions.

TABLE III. ELASTIC CONSTANTS

Elastic Constants	Cross-Linked Nanotube Fiber (GPa)	Nanotube Bundle Without Cross-Links (GPa) [3]
C_{11}	350	570
K_{12}	80	11
K_{23}	2.7	24
G_{12}	3.7	35
G_{23}	0.84	1

The Young's and shear moduli of the embedded, cross-linked nanotube effective fiber in the polyimide LaRC-SI are plotted in Figure 3 as a function of nanotube volume fraction for randomly orientated fibers. Both the Young's and shear modulus show monotonic increases with increasing nanotube volume fraction.

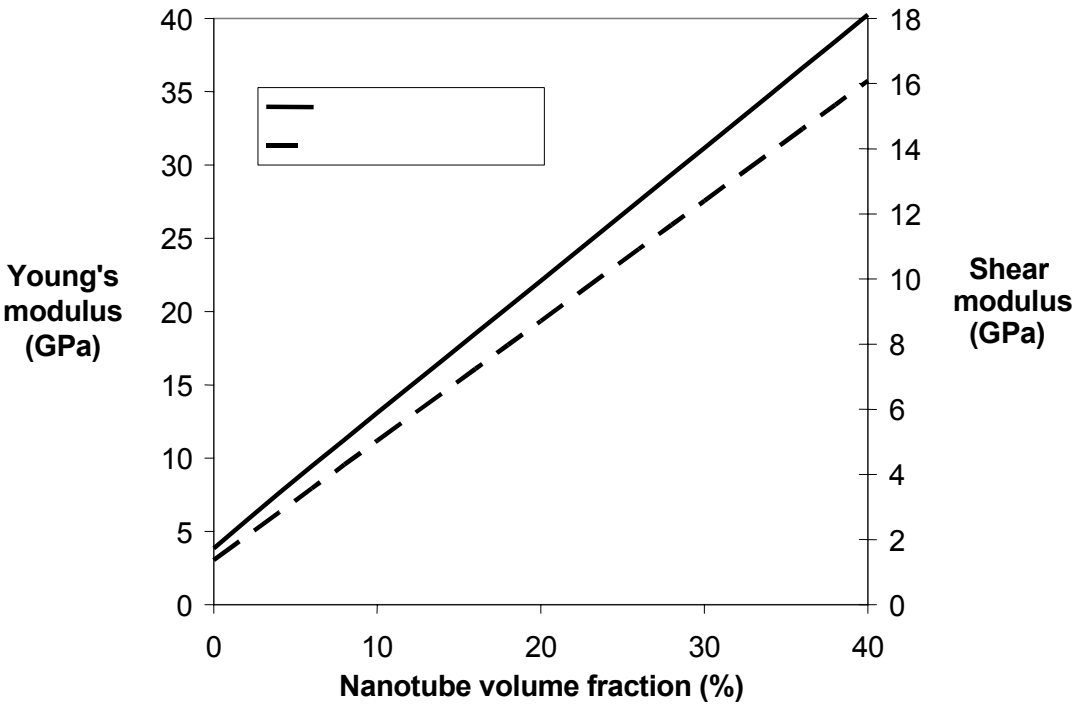

Figure 3. Elastic constants of the cross-linked nanotube/LaRC-SI Composite.

CONCLUSIONS

The constitutive properties of single-walled carbon nanotubes cross-linked with a variable stiffness tethers were determined with a multi-scale modeling method. The method used molecular dynamics simulation and equivalent continuum modeling to determine the elastic constants. Input for the force field used in the molecular dynamics simulations was customized for the cross-linker with *ab initio* calculations. It is assumed that the material was transversely isotropic, and therefore, five independent constants were determined. A comparison of the constants with similarly derived ones for a nanotube bundle without any cross-linker demonstrated that the mechanical properties are affected by the separation of the nanotubes in the bundles, and by the cross-linker having multiple degrees of freedom giving it the capability of absorbing some of the strain energy. The effect of the cross-linked nanotubes in increasing the Young's and shear moduli of a composite with increasing nanotube

volume fraction is demonstrated by modeling the nanotubes as effective fibers in a polyimide with a micromechanical analysis.

REFERENCES

1. Gates, T. S. and J. A. Hinkley. 2003. "Computational Materials: Modeling and Simulation of Nanostructured Materials and Systems," NASA Langley Research Center, Hampton, VA. NASA/TM-2003-212163.
2. Thostenson, E. T., Z. F. Ren, and T. W. Chou. 2001. "Advances in the science and technology of carbon nanotubes and their composites: a review," Composites Science and Technology, 61:1899-1912.
3. Odegard, G. M., S. J. V. Frankland, M. N. Herzog, T. S. Gates, and C. C. Fay. April 2004. "Constitutive Modeling of Crosslinked Nanotube Materials," presented at the 45th AIAA/ASME/ ASCE/AHS/ASC Structures, Structural Dynamics, and Materials Conference, Palm Springs, CA. AIAA-2004-1606.
4. Frankland, S. J. V., M. N. Herzog, G. M. Odegard, T. S. Gates, and C. C. Fay. 2003. "Modeling and Characterization of Elastic Constants of Functionalized Nanotube Materials," *MRS Symposium Proceedings*. Boston, MA; Materials Research Society.
5. Levine, I. N. 1991. *Quantum Chemistry,* Prentice-Hall, Inc., Englewood Cliffs, NJ. Ch.11, 15, 17.
6. R. J. Harrison, J. A. Nichols, T. P. Straatsma, M. Dupuis, E. J. Bylaska, G. I. Fann, T. L. Windus, E. Apra, W. de Jong, S. Hirata, M. T. Hackler, J. Anchell, D. Bernholdt, P. Borowski, T. Clark, D. Clerc, H. Dachsel, M. Deegan, K. Dyall, D. Elwood, H. Fruchtl, E. Glendening, M. Gutowski, K. Hirao, A. Hess, J. Jaffe, B. Johnson, J. Ju, R. Kendall, R. Kobayashi, R. Kutteh, Z. Lin, R. Littlefield, X. Long, B. Meng, T. Nakajima, J. Nieplocha, S. Niu, M. Rosing, G. Sandrone, M. Stave, H. Taylor, G. Thomas, J. van Lenthe, K. Wolinski, A. Wong, and Z. Zhang. 2002. "NWChem, A Computational Chemistry Package for Parallel Computers, Version 4.1," Pacific Northwest National Laboratory, Richland, Washington.
7. Cornell, W.D., P. Cieplak, C. I. Bayly, I. R. Gould, K. M. Merz, D. M. Ferguson, D. C. Spellmeyer, T. Fox, J. W. Caldwell, and P. A. Kollman. 1995. "A Second Generation Force Field for the Simulation of Proteins, Nucleic Acids, and Organic Molecules." *Journal of the American Chemical Society*. 117:5179-5197.
8. Smith, W. and Forester, T.R. 1996. DL-POLY, Warrington, England: The Council for the Central Laboratory of the Research Councils.
9. Hashin Z. and B. W. Rosen. 1964. "The Elastic Moduli of Fiber-Reinforced Materials," Journal of Applied Mechanics, June:223-232.
10. Mori, T. and K. Tanaka. 1973. "Average Stress in Matrix and Average Elastic Energy of Materials with Misfitting Inclusions," *Acta Metallurgica*, 21:571-574.
11. Benveniste, Y. 1987. "A New Approach to the Application of Mori-Tanaka's Theory in Composite Materials," *Mechanics of Materials*. 6:147-157.
12. Eshelby, J.D. 1957. "The Determination of the Elastic Field of an Ellipsoidal Inclusion, and Related Problems," *Proceedings of the Royal Society of London, Series A*., 241:376-396.
13. Whitley, K.S., T. S. Gates, J. Hinkley, and L. M. Nicholson. 2000. "Mechanical Properties of LaRC™ SI Polymer for a Range of Molecular Weights," NASA Langley Research Center, Hampton, VA. NASA/TM-2000-210304.